



INVESTIGATION OF AERODYNAMIC AND AEROACOUSTIC PERFORMANCE OF CROSS FLOW FANS

Özgür BAYRAKDAR¹, Cem DEMİRKESEN¹,
Esra SORGÜVEN², İlhami GÜMÜŞ¹

¹ *Vestel Beyaz Esya A.S., Manisa OSB Vestel City Air Conditioner Plant
R&D Department 45030 Manisa, Turkey*

² *Department of Mechanical Engineering, Yeditepe University,
Kayışdağı Istanbul, Turkey*

SUMMARY

Purpose of this study is to investigate how the impeller geometry influences the aerodynamics and aeroacoustics of a cross flow fan. In a cross flow fan, air flows through the impeller, which generates an eccentric vortex within the blade row. In this study, the impeller geometry is modeled with four parameters. Design of experiments method is used to generate a well-distributed set of parameters, which can be used for surface fitting. Accordingly, 24 CFF geometries are determined and the corresponding CFD simulations are performed. Flow data are evaluated to predict the acoustic and aerodynamic performance. Results show that the influence of the impeller geometry on the overall acoustic and aerodynamic performance is not as large as in axial or radial fans because of the vortex-dominated flow through the cross flow fan. Via the impeller optimization average vorticity can be decreased by ca. 8% without adversely affecting the pressure head. The most influential geometrical features of a CFF impeller are the outer blade diameter and the chord length. Future work of this study is to produce the optimum impeller via rapid prototyping and to measure its aerodynamic and acoustic performance.

INTRODUCTION

Cross flow fan (CFF) is a vital component of an indoor air conditioning unit. CFFs are preferred over axial or radial flow fans in indoor air conditioning units (Fig. 1, Fig. 2), since these provide higher air flow rates at relatively low noise levels. For the air conditioner industry, cross flow fan (CFF) design is important to assure an efficient heat transfer from the heat exchanger and also to reduce the overall sound pressure level of the indoor air-conditioning unit. Air flow and noise

generation mechanisms in a CFF are fundamentally different than axial or centrifugal fans. In a CFF, air flows through the impeller, which causes that both ends of each blade switch from leading to trailing edge throughout one rotation. The flow structure inside the fan consists of two regions: the through-flow region and the eccentric vortex region. Efficiency of a CFF is fundamentally limited by the unavoidable eccentric vortex within the impeller. Furthermore, this recirculation zone makes the analysis of this type of fans very complicated. Analytic studies on CFFs began with Eck [1], who described the flow inside the impeller as a potential flow with vorticity sources located in the blade row near the vortex wall. Most of the analytical studies on CFFs rely on the potential flow theory [2-4]. The position and the extend of the eccentric vortex depends on the geometrical features of both the impeller and the casing, as well as the operating conditions, i.e. mass flow rate, rotational speed and pressure head. Even though there are semi-empirical methods to predict aerodynamic and aeroacoustic properties of axial or radial fans, to develop such reliable semi-empirical methods for CFFs has proven to be very difficult. Numerical and experimental studies about cross flow fans (CFF) are scarce in the literature [5, 6], especially the ones where numerical calculations are validated with experimental measurements [7].

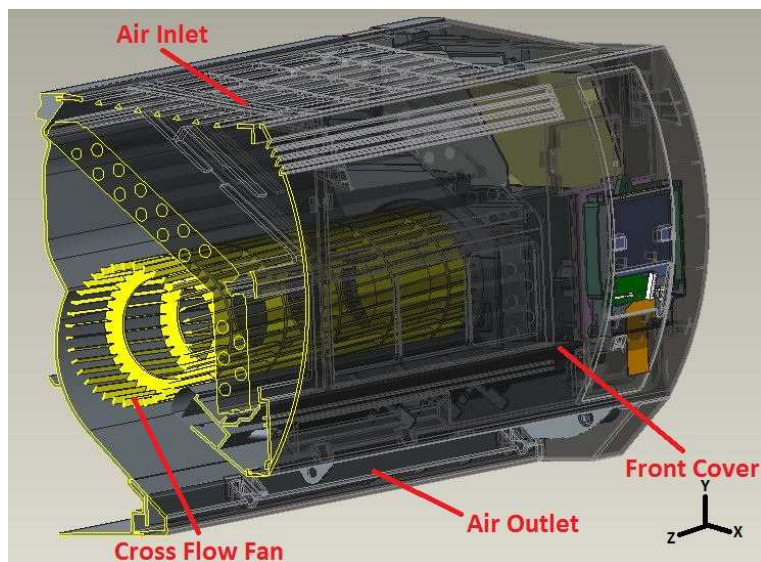


Figure 1: Geometry of cross flow fan in split type air conditioner indoor unit

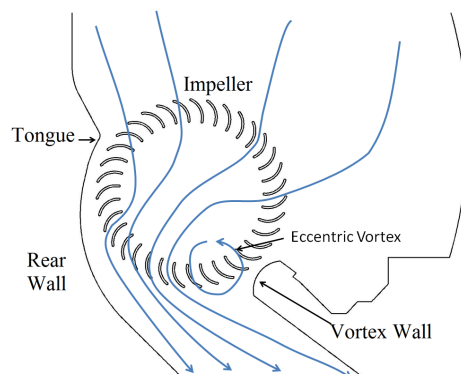


Figure 2: Details of a cross flow fan

Design of the impeller affects acoustic and aerodynamic performance of the CFF dramatically. Our preliminary studies showed that impellers, having the same outer diameter and operating in the same casing with the same rotational speed, result in a large variation both in the aerodynamic and

acoustic performance. In the measurements overall sound power level changed in a range of 40 to 50 dB(A) and the flow rate changed in a range of 600 to 800 m³/h. This flow rate difference can change the seasonal coefficient of performance (SCOP) up to 0.5, which can result in a quieter air-conditioning unit in a higher energy class.

The aim of this study is to investigate the effect of geometric features of the impeller on the aerodynamic and aeroacoustic performance. Geometry of the impeller is described via 4 parameters, i.e. blade angles and radii. To understand the linear and non-linear relationships between the geometrical and aerodynamic variables, parameters are varied systematically and numerical simulations are performed. Results of the simulations are evaluated to gain insight on the correlations between the geometrical and aerodynamic variables. Response surfaces are obtained and an optimization with two goals, namely maximizing the aerodynamic performance and minimizing the noise level is performed.

GEOMETRY OF THE INVESTIGATED CFF

Previous studies showed that the parameters having an impact on the flow characteristics in a CFF are impeller and casing geometry, flow rate, pressure head and rotational speed. There is a strong non-linear interaction between these parameters. Even small changes in these parameters may result in dramatic changes in the overall performance of the CFF [6]. This study focuses only on the effect of the impeller geometry on the CFF flow. The geometry of the casing is kept the same, as well as the total flow rate and the rotational speed of the CFF. The geometry of the impeller is defined via four geometric parameters as shown in Fig. 3: inner blade angle (β_1), outer blade angle (β_2), outer blade radius (d_2) and the outer radius - inner radius ratio (d_2/d_1). To evaluate the effects and possible interactions between these geometric parameters on the aerodynamics and acoustics of the CFF, values of the parameters are systematically varied and new impeller geometries are generated. Since a full factorial design would result in an unfeasibly large number of geometries, design of experiments (DoE) is employed. Table 1 shows the parameter sets of the 24 impeller geometries calculated via DoE.

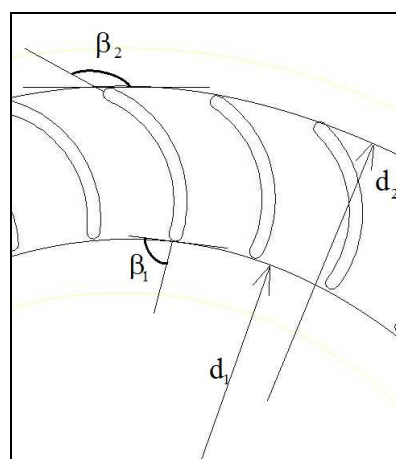


Figure 3: Geometric parameters of the impeller

Table 1: Parameters of the investigated fans

	β_1	β_2	d_1/d_2	d_2
Fan 1	80	150	0.78	91
Fan 2	80	160	0.78	91
Fan 3	90	150	0.78	91
Fan 4	90	160	0.78	91
Fan 5	85	155	0.75	86
Fan 6	85	155	0.75	96
Fan 7	85	155	0.82	86
Fan 8	85	155	0.82	96
Fan 9	80	155	0.78	86
Fan 10	80	155	0.78	96
Fan 11	90	155	0.78	86
Fan 12	90	155	0.78	96
Fan 13	85	150	0.75	91
Fan 14	85	150	0.82	91
Fan 15	85	160	0.75	91
Fan 16	85	160	0.82	91
Fan 17	80	155	0.75	91
Fan 18	80	155	0.82	91
Fan 19	90	155	0.75	91
Fan 20	90	155	0.82	91
Fan 21	85	150	0.78	86
Fan 22	85	150	0.78	96
Fan 23	85	160	0.78	86
Fan 24	85	160	0.78	96

NUMERICAL SIMULATIONS

Numerical simulations for the 24 CFFs are performed with the commercial CFD software Fluent using the k-epsilon RNG (Re-normalization Group Theory) method which is an appropriate RANS model for low Reynold and swirl-dominated flows. The governing equations for the turbulence modeling are:

$$\frac{\partial}{\partial t}(\rho k) + \frac{\partial}{\partial x_i}(\rho k u_i) = \frac{\partial}{\partial x_j} \left(\alpha_k \mu_{eff} \frac{\partial k}{\partial x_j} \right) + G_k + G_b - \rho \varepsilon - Y_M + S_K \quad (1)$$

$$\frac{\partial}{\partial t}(\rho \varepsilon) + \frac{\partial}{\partial x_i}(\rho \varepsilon u_i) = \frac{\partial}{\partial x_j} \left(\alpha_s \mu_{eff} \frac{\partial \varepsilon}{\partial x_j} \right) + C_{1s} \frac{\varepsilon}{k} (G_k + G_{3s} G_b) - C_{2s} \rho \frac{\varepsilon^2}{k} - R_s + S_s \quad (2)$$

Where,

G_k : Generation of turbulence kinetic energy due to mean velocity gradients

G_b : Generation of turbulence kinetic energy due to buoyancy

Y_M : Contribution of the fluctuating dilatation in compressible turbulence to the overall dissipation rate

α_k : Inverse effective Prandtl numbers for k

α_ε : Inverse effective Prandtl numbers for ε

S_k : User-defined source term

The scale elimination procedure in RNG theory results in a differential equation for turbulent viscosity:

$$d\left(\frac{\rho^2 k}{\sqrt{\varepsilon\mu}}\right) = 1.72 \frac{\hat{\nu}}{\sqrt{\hat{\nu} - 1 + c_\nu}} d\hat{\nu} \quad (3)$$

where, $\hat{\nu} = \mu_{eff} / \mu$, and $c_\nu \approx 100$.

CFF geometry is modeled as a 2-dimensional surface normal to the rotation axis. Validity of the 2D assumption is guaranteed via stereoscopic PIV measurements performed by Kumlutaş et al. [8] for similar CFFs. PIV results for the baseline CFF shows that the measured axial velocities are less than 10% of the mean flow velocity in the entire flow field.

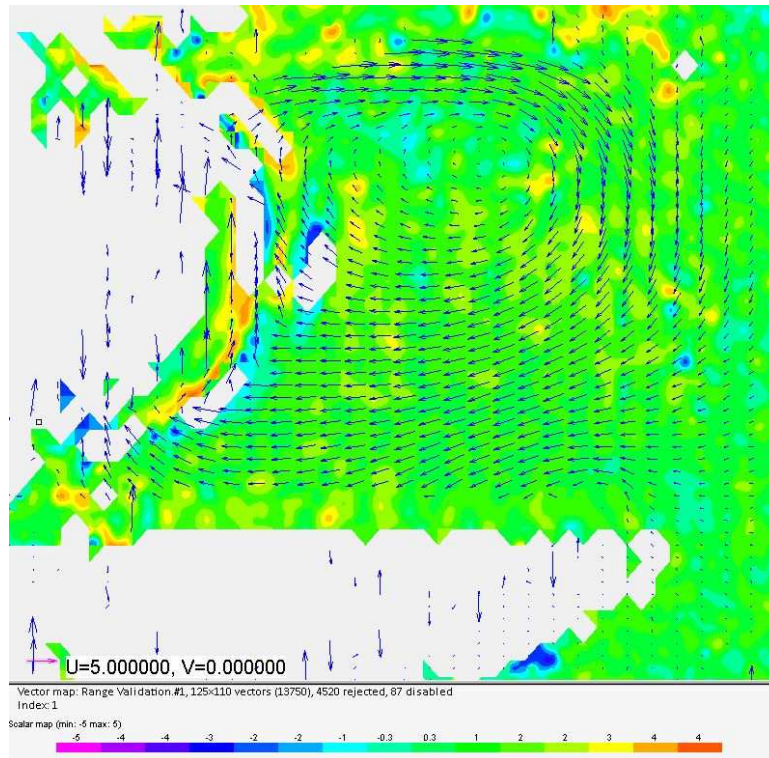


Figure 4: Stereoscopic PIV measurement of the baseline CFF
(Contours are plotted for the velocity component normal to the rotation axis)

In all simulations the same physical and numerical models are employed. At the inlet boundary, uniform velocity profile with an average velocity of 1.25 m/s is set. At the outlet boundary pressure is kept constant. Mesh consists of two zones: stationary and rotating. Steady state simulations are performed, where the impeller rotation is simulated via frame motion. The stationary zone is bounded by the casing walls and a circular interface with the rotating zone. The mesh for the stationary zone is kept the same in each simulation. The second zone is the rotating zone surrounding the impeller blades. The mesh topology and the meshing strategy are kept the same for the rotating zone, so that each simulation bears similar discretization errors. Figure 5 shows one of the computational meshes, which contain in the average 220.000 control volumes.

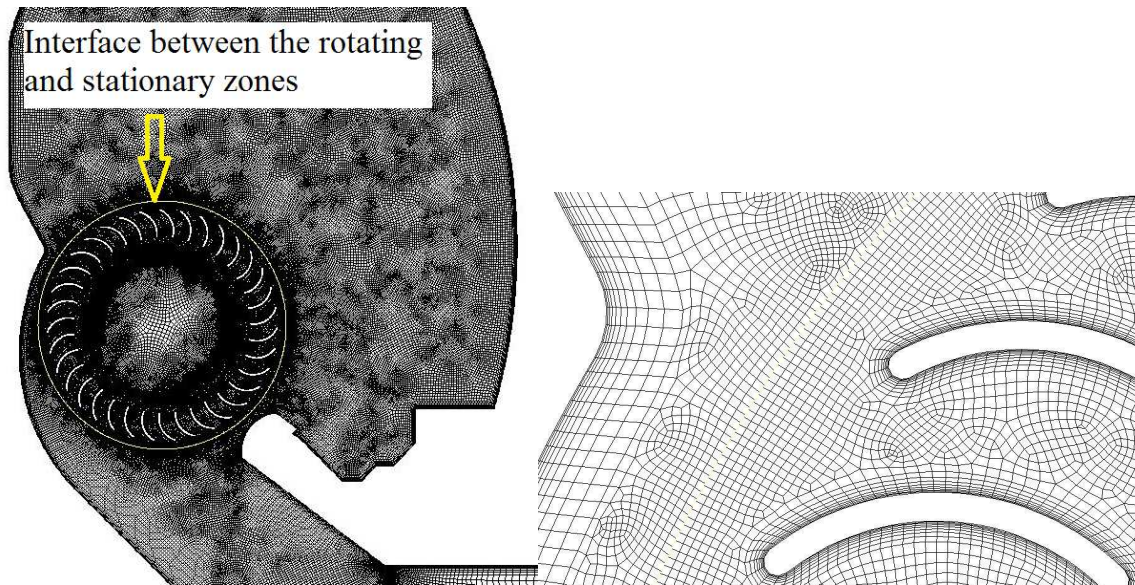


Figure 5: Computational mesh of the baseline CFF

Simulation methodology is validated by comparing the numerical results of the baseline design with the PIV measurements. Figure 6 shows the comparison of the numerical and experimental streamlines, and figure 7 shows the velocity profiles on a line in the discharge region.

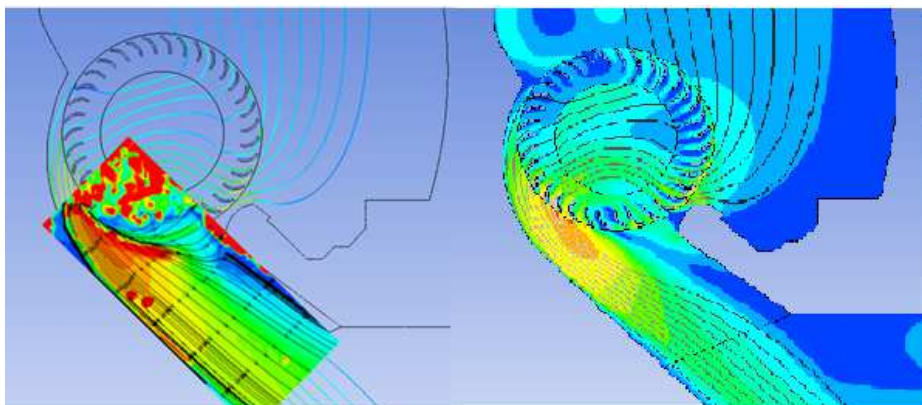


Figure 6: Comparison of the numerical results with the PIV measurements for the baseline design

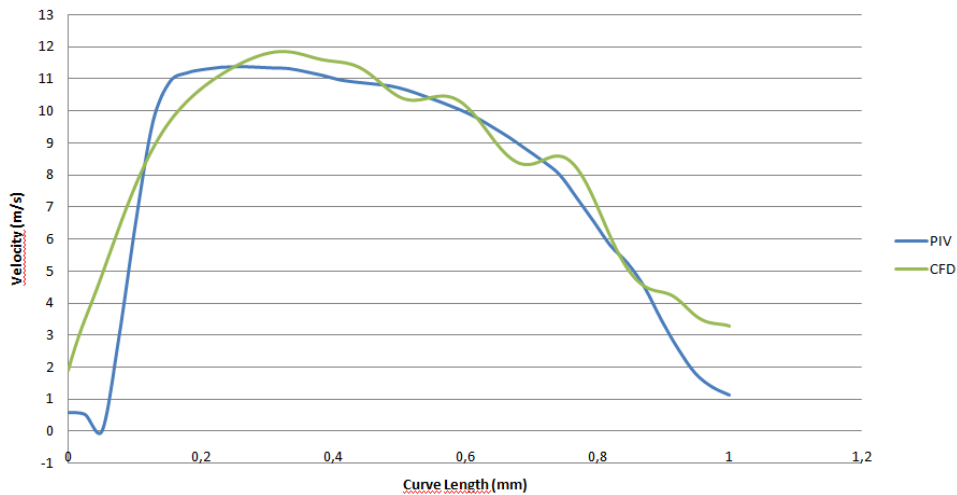


Figure 7: Graphical comparison of the numerical results with the PIV measurements for the baseline design

Results of the Numerical Simulations

The CFD results of the baseline geometry show that there are two main vortices in the investigated CFF. One is the eccentric vortex, which appears within the blade row adjacent the vortex wall. The other vortex appears upstream the flow near the rear wall. The upstream vortex blockades the impeller inlet area partially, so that the streamlines inside the impeller become horizontal. The size and location of the upstream vortex is primarily affected by the rear wall. By changing the rear wall geometry, the upstream vortex size could be decreased. If the gap between the casing and the impeller blades would be decreased, for example with the help of a tongue geometry, than this upstream vortex can be eliminated. However, since this study is focused on the impeller geometry, rear wall geometry is kept as it is and the effects of the impeller parameters on the vortices are investigated.

In the baseline geometry, inflow to the impeller occurs towards the vortex wall and outflow from the impeller occurs towards the rear wall. About half of the impeller circumference is blockaded via the two vortices. Since the outflow region is limited, flow velocities at the impeller outlet increase up to 20 m/s (Fig. 8a). Fig. 8b shows that the vorticity is generated via the eccentric vortex, as well as the boundary layers on the blade surfaces, vortex and rear walls.

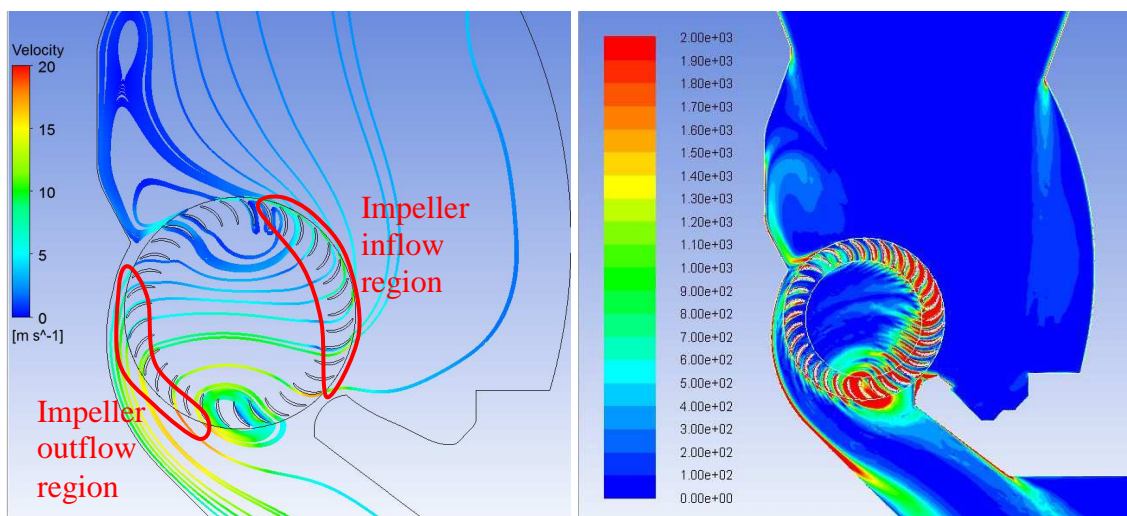


Figure 8a: Streamlines (baseline design)

Figure 8b: Vorticity contours (baseline design)

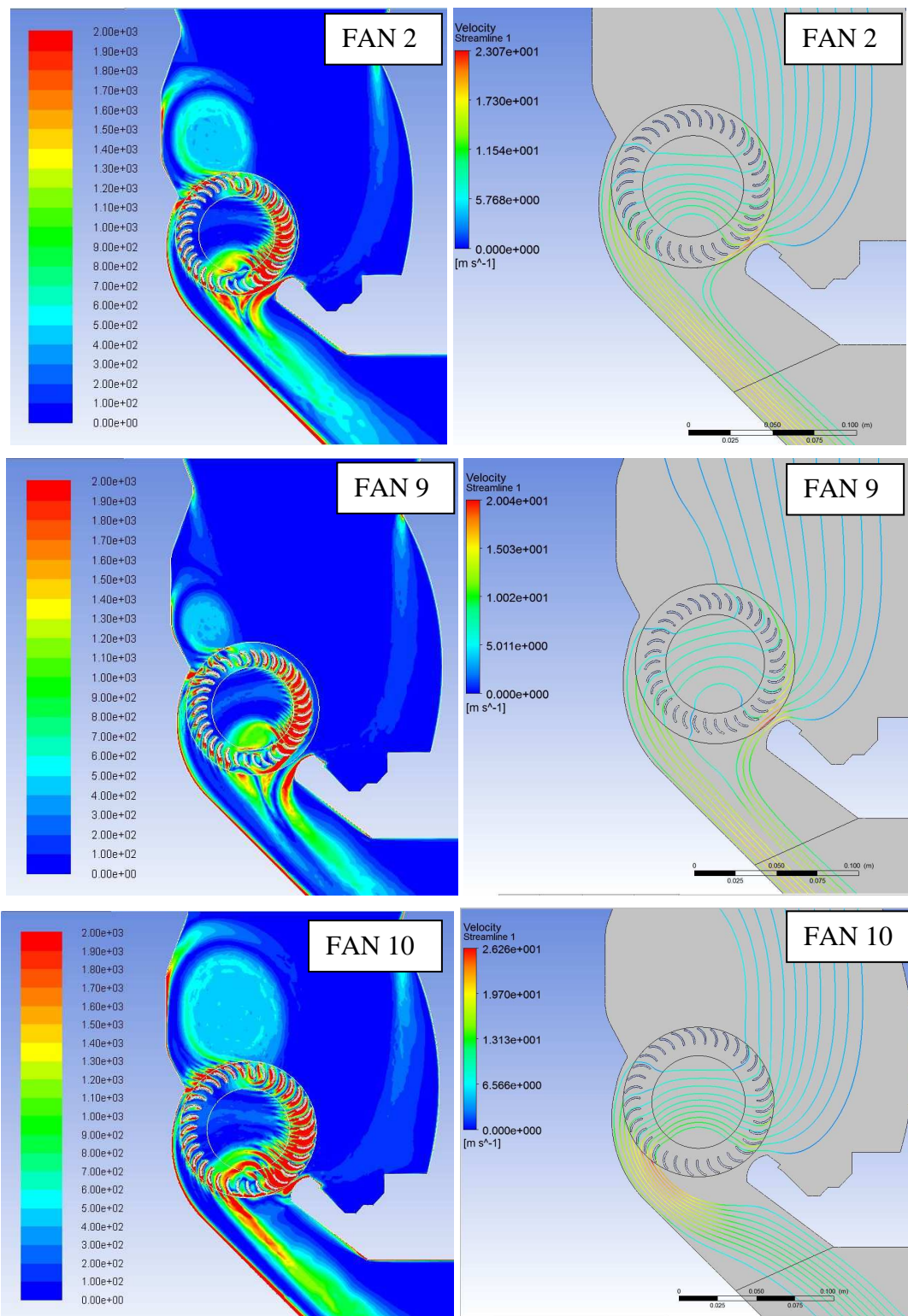


Figure 9: Vorticity contours and streamlines and of CFFs 2 (top), 9(middle) and 10(bottom)

Figure 9 shows vorticity contours and streamlines of the three of the investigated CFFs. In all of the CFFs, vorticity is generated by the eccentric and upstream vortices as well as the blade surfaces, vortex and rear wall boundary layers. Vorticity is convected towards the discharge with the main flow. In some of the investigated CFF geometries, a leakage flow between the impeller blades and the vortex wall occurs (see CFF 2 and 9 in Fig. 9). This leakage occurs especially when the gap

between the blades and vortex wall is large, i.e. in geometries with low outer radii. The position and extend of the eccentric vortex also effects the upstream vortex size (Fig. 9). Especially outer blade radius d_2 and angle β_2 have an effect on the upstream vortex size.

Several flow variables are extracted from the simulations and their correlations with the impeller parameters are investigated. Table 2 summarizes some of the important correlations. Total pressure increase across the impeller is an indication on the fan performance. Since the mass flow rate is kept constant in the simulations, the fan with the highest pressure increase can be regarded as the one with the highest aerodynamic efficiency. A correlation of 0.88 proves that the outer impeller diameter has the highest impact on the pressure increase.

Vorticity and pressure standard deviation on casing walls are indicators of the power of noise sources, especially dipoles [9]. Area-weighted vorticity averages on flow domains and pressure standard deviation on the vortex wall are also strongly correlated with the outer blade diameter.

Table 2: Correlations between the impeller parameters and some of the flow variables

	ΔP_{total} (Pa)	Average vorticity on the rotating zone (1/s)	Average vorticity on the stationary zone (1/s)	Pressure standard deviation on the vortex wall (Pa)	Moment (N.m)
β_1	-0.12	-0.03	-0.40	-0.25	-0.27
β_2	0.17	0.29	0.18	0.04	-0.01
d_1/d_2	-0.17	-0.41	-0.36	-0.41	-0.18
d_2	0.88	0.85	0.37	0.75	0.90

OPTIMIZATION

Goal of the optimization is to minimize the power of the noise sources in the flow field while maximizing the aerodynamic efficiency. For this purpose the following two optimization objectives are formulated:

- Minimize the average vorticity on the rotating zone
- Maximize the total pressure increase

Unfortunately, the correlations in Table 2 show that those are competitive goals. For example, any increase in the outer blade diameter d_2 , would cause an increase in the total pressure increase (hence, a higher aerodynamic efficiency); but also increases the generated vorticity. Hence, more powerful dipole source would be generated.

The present optimization requires simultaneous minimization of two flow variables. In contrast to single objective optimization problems, the solution of this multi-objective optimization is not a single point, but a family of points referred to in the literature as Pareto points or Pareto front [10]. An example to explain the theory of Pareto front is the 1-variable 2-objectives problem used in [11]. Objectives of this problem are:

- Minimize $f_{11} = x^2$
- Minimize $f_{12} = (x-2)^2$

Any point between 0 and 2 can be a solution for this problem. So, here the Pareto front is $\{x|0 \leq x \leq 2\}$

Response surface methodology is used to explore the relationships between the extracted flow variables and the geometric parameters. Both the average vorticity on the rotating zone and the total pressure increase are described as polynomial functions of the impeller parameters $\beta_1, \beta_2, d_1/d_2, d_2$. The software Matlab is used to calculate the constants of the polynomial functions. Multi-objective optimization is performed with Matlab's gamultiobj function. Optimization resulted in 21 Pareto designs, and 6 of these Pareto designs are chosen for further study. CFD analyses are performed for the chosen six CFFs. The average vorticity and the total pressure increase calculated for the Pareto optimum CFFs are plotted in Fig. 10.

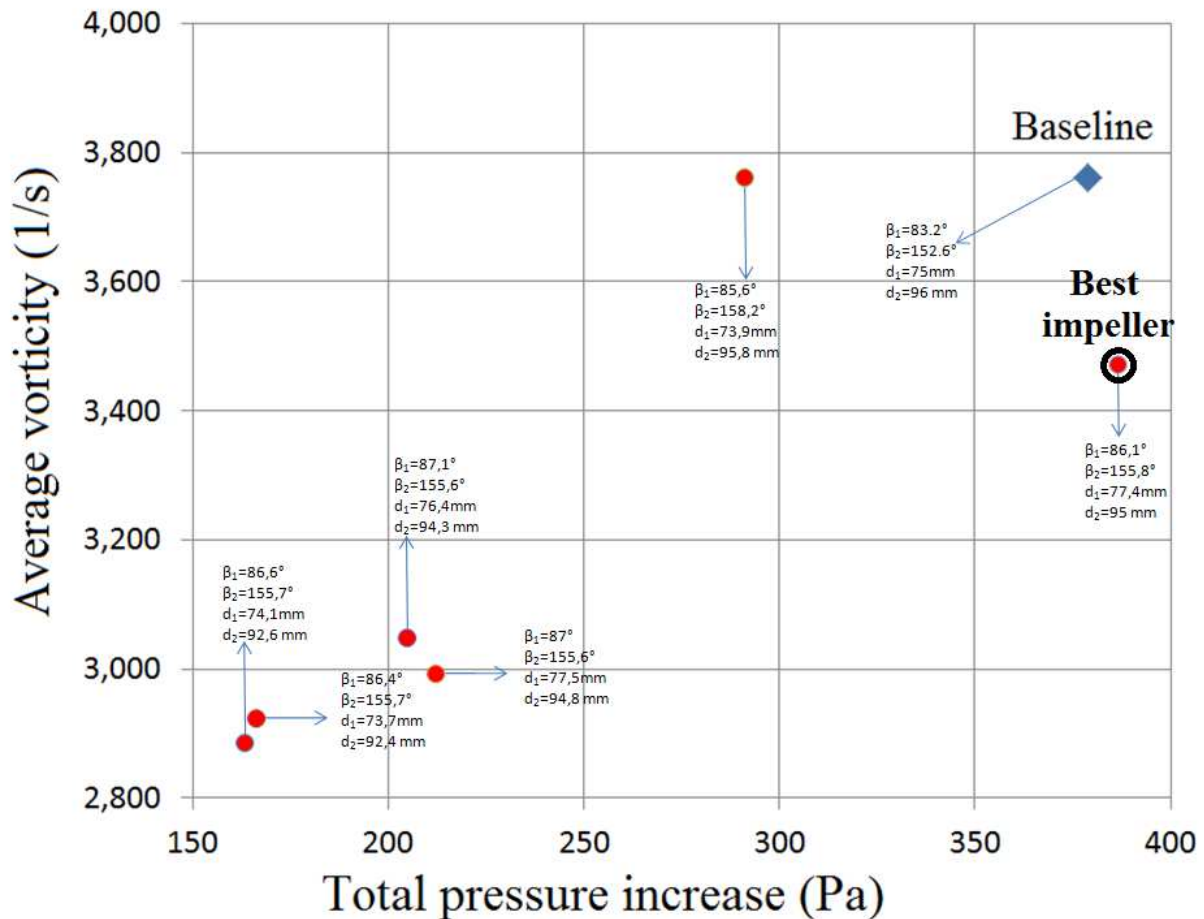


Figure 10: CFD results of the Pareto optimum designs (denoted with red dots) vs. the baseline design (denoted with the blue diamond)

First conclusion that we can deduce from these results is that, the effect of the impeller geometry alone has only a limited effect on the overall performance of a CFF. The geometry of a CFF impeller is very similar to the impeller of a Sirocco fan. Sirocco fans are radial fans with 30-40 blades having short chord lengths, just like CFF impellers. A previous parametric CFD study of a Sirocco fan showed that by changing the impeller parameters only (keeping the stator geometry the same) the average vorticity could be decreased ca. 30% without adversely affecting the pressure head [9]. Here, the best impeller can decrease the average vorticity by 8% without adversely affecting the pressure head. Even though the impeller geometries of Sirocco and CFF fans are very similar, since the flow through a Sirocco impeller is radial, flow characteristics are completely different. These results show that the influence of the blade geometry on the flow across a CFF is limited.

Figure 10 shows that all 6 Pareto designs have similar blade angles. For all of the Pareto designs β_1 is nearly 86° and β_2 is nearly 156° . Inner and outer blade diameters exhibit a larger variation.

Impellers with a smaller outer diameter result in a lower vorticity and lower pressure head. Impellers with larger outer diameter generate generally a higher pressure head but also a higher vorticity, except for the best design.

CFD results show that only one of the Pareto optimum designs result in a higher pressure increase and a lower vorticity generation. This fan is indicated as the “best design” in figure 10 and has the following geometric parameters: $\beta_1=86.1^\circ$, $\beta_2=155.8^\circ$, $d_1=77.4$ mm, and $d_2=95$ mm. The streamlines, vorticity distribution and total pressure contours for this CFF are shown in the figure below.

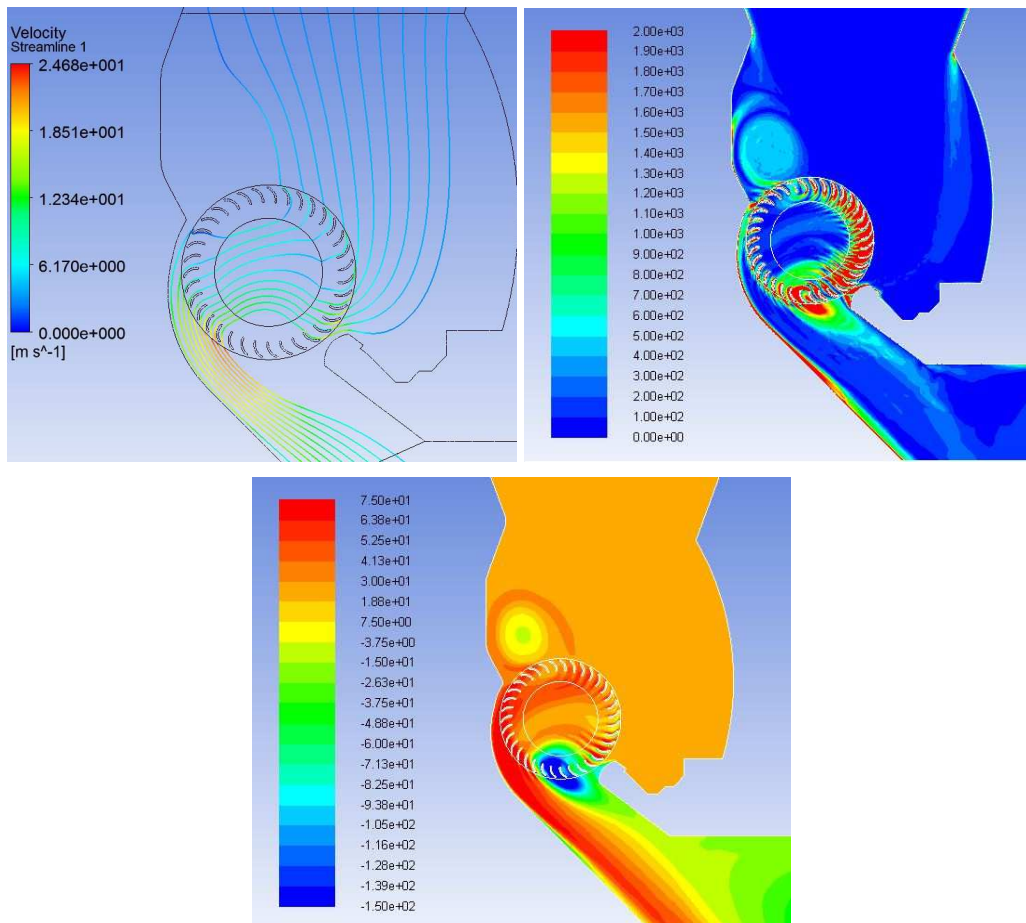


Figure 11: CFD results of the best Pareto optimum design

The best design impeller manages to provide a slightly higher pressure head than the baseline design, even though it has a smaller outer diameter. The chord length of the best design is 16% shorter than the baseline design ($l_{\text{baseline}}=21\text{mm}$, $l_{\text{best design}}=17.6$ mm). In fact, five out of the total six Pareto designs have shorter chord lengths than the baseline design. The chord length of these 5 Paretos are nearly the same, even though their outer diameter differ. One conclusion that we can draw here is that, the chord length (or the blade surface area) plays an important role on the aerodynamic and aeroacoustic performance of a CFF.

CONCLUSION

In the frame of this work, a multi-objective optimization of a CFF is performed. The sole input of the optimization procedure is the flow data extracted from steady RANS simulations. Since hardware and computation time requirements for steady RANS simulations are low, optimization can be performed with reasonable resources. As a result of this optimization one CFF impeller geometry is determined, which produces a higher pressure increase and a lower vorticity than the baseline impeller.

This study shows that the average vorticity in a CFF can be decreased by ca. 8% by improving the impeller blade geometry. This improvement rate is not as high as in axial or radial fans; because, in a CFF flow is dominated by the eccentric vortex and the impeller has a limited effect on the overall flow characteristics.

Another result of this study is that the most important geometrical features of a CFF impeller are the outer blade diameter and the chord length. The other investigated parameters, i.e. the blade angles converge to unique optimum values, which remain the same for each Pareto design.

Future work of this study is to produce the optimum impeller via rapid prototyping and to measure its aerodynamic and acoustic performance.

REFERENCES

- [1] Eck B. *Fans*. Oxford: Pergamon Press; **1973**.
- [2] Coester R. *Theoretische und experimentelle Untersuchungen an Querstromgeblase. Mitteilungen aus dem Institut für Aerodynamik ETH*. **1959**. p. 28.
- [3] Tramposch H. *Cross-flow fan*. ASME Paper No. 64-WA/FE-25. **1964**.
- [4] Ilberg H, Sadeh WZ. *Flow theory and performance of tangential fans*. In: *Proceedings of the Institution of Mechanical Engineers*, vol. 180. **1965**. p. 481–96.
- [5] A. Toffolo, A. Lazzaretto, A.D. Martegani, *An experimental investigation of the flow field pattern within the impeller of a cross-flow fan*, *Experimental Thermal and Fluid Science* 29, 53-64, **2004**.
- [6] L. Lazzarotto, A. Lazzaretto, A. D. Martegani, A. Macor, *On Cross-Flow Fan Similarity: Effects of Casing Shape*, *Journal of Fluids Engineering*, 123, 523 – 531, **2001**.
- [7] A. Toffolo, *On the theoretical link between design parameters and performance in cross-flow fans: a numerical and experimental study*, *Computers & Fluids* 34, 49–66, **2005**.
- [8] Kumlutaş, D., Karadeniz, Z.H., *Investigation of flow and heat transfer for a split air conditioner indoor unit*, *Applied Thermal Engineering*, 51, 262-272, **2013**.
- [9] E. Sorgüven, Y. Dogan, *Acoustic optimization for centrifugal fans*, *Noise Control Engineering Journal*, 60 (4), 379-391, **2012**.
- [10] P. Sen, J.B. Yang, *Multiple Criteria Decision Support in Engineering Design*, Springer, London, **1998**.
- [11] T.L. Vincent, G.J. Grantham, *Optimality in parametric systems*, John Wiley and Sons, New York, **1981**.